

## Pump-probe spectroscopy and velocimetry of cold atoms in a slow beam

G. Di Domenico, G. Mileti, and P. Thomann

Observatoire Cantonal, rue de l'Observatoire 58, CH-2000 Neuchâtel, Switzerland

In this paper we report on the first purely “pump-probe” nonlinear laser spectroscopy results in a slow atomic beam. We have observed Raman, Rayleigh, and recoil-induced resonances (RIR) in a continuous beam of slow and cold cesium atoms extracted from a two-dimensional (2D) magneto-optical-trap (MOT) with the moving molasses technique. The RIR enabled us to measure the velocity distribution, therefore the average speed (0.6–4 m/s) and temperature (50–500  $\mu\text{K}$ ) of the atomic beam. Compared to time of flight, this technique has the advantage of being local, more sensitive in the low-velocity regime ( $v < 1$  m/s), and it gives access to transverse velocities and temperatures. Moreover, it may be extended to measure atomic velocities in the 2D MOT source of the atomic beam.

### I. INTRODUCTION

Pump-probe spectroscopy is a powerful tool for high resolution measurements and to get information on laser-cooling mechanisms [1–6]. In particular one can measure atomic velocity distributions by using the recoil-induced resonance (RIR) [7]. This technique has been demonstrated either in a cloud of cold atoms in the dark [8] or in a one-dimensional (1D) molasses [9]. In both situations the average velocity of the atomic sample was zero ( $\bar{v} = 0$ ).

We have used the same technique to measure the velocity distribution in a beam of cold atoms where  $\bar{v} \neq 0$ . The continuous beam is produced with a two-dimensional (2D) magneto-optical trap (MOT) operating as a moving molasses in the vertical direction [10]. The atoms are launched downward and the velocity distribution measurement takes place in the atomic beam under the source.

A simple description of the physical principle underlying recoil-induced resonances is as follows. Two laser beams, a pump beam of frequency  $\omega$  and wave vector  $\vec{k}$  and a probe beam of frequency  $\omega_p = \omega + \delta\omega$  and wave vector  $\vec{k}_p$ , cross an ensemble of free atoms at an angle  $\theta$  [Fig. 1(a)]. Their detuning from the atomic resonance is larger than the natural width of the excited state  $\omega_{\text{atom}} - \omega > \Gamma$  but their mutual detuning is much smaller  $|\delta\omega| \ll \Gamma$ . They have parallel linear polarizations and the angle  $\theta$  is chosen sufficiently small to have  $|\vec{k}_p - \vec{k}| \approx k\theta$  where  $k = |\vec{k}| \approx |\vec{k}_p|$ . The RIR appears on the transmission spectrum of the probe beam. It can be interpreted in terms of a stimulated Raman process between two different momentum states [Fig. 1(b)]. Indeed, the momentum states  $p_z$  and  $p_z + \hbar k\theta$  are coupled by two competing processes. The first one, absorption from the probe followed by stimulated emission into the pump, attenuates the probe whereas the second one, absorption from the pump followed by stimulated emission into the probe, amplifies the probe. The resulting variation of the probe intensity is thus proportional to the population difference of the two momentum states  $\Delta I_p/I_p \propto \pi(p_z + \hbar k\theta) - \pi(p_z)$ . This is nothing but the derivative of the momentum distribution as long as  $\pi(p_z)$

varies slowly on any interval of width  $\hbar k\theta$ . Moreover, the resonance condition  $p_z = M\delta\omega/k\theta$  shows that we can select the momentum class of the atoms undergoing the Raman transition by choosing the pump-probe detuning  $\delta\omega$ . Therefore the transmission spectrum of the probe beam is proportional to the derivative of the momentum distribution,

$$\frac{\Delta I_p}{I_p}(\delta\omega) \propto \frac{d\pi}{dp_z}(M\delta\omega/k\theta). \quad (1)$$

In the case of a thermal cloud, the momentum distribution is a Gaussian, therefore the transmission spectrum displays a dispersionlike curve centered at  $\delta\omega = 0$  whose distance between peaks is  $2k\theta\sqrt{k_b T/M}$ .

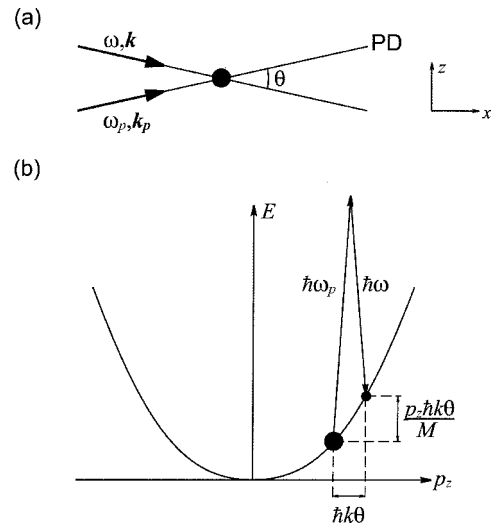


FIG. 1. Recoil-induced resonance. (a) Scheme of the laser beams. (b) Stimulated Raman transition between momentum states  $p_z$  and  $p_z + \hbar k\theta$ . For  $\delta\omega = \omega_p - \omega$  fixed, energy and momentum conservation imply that only atoms with  $p_z = M\delta\omega/k\theta$  are resonantly excited. The variation of probe intensity is proportional to the population difference of the two momentum states (populations are represented by the circles' diameters).

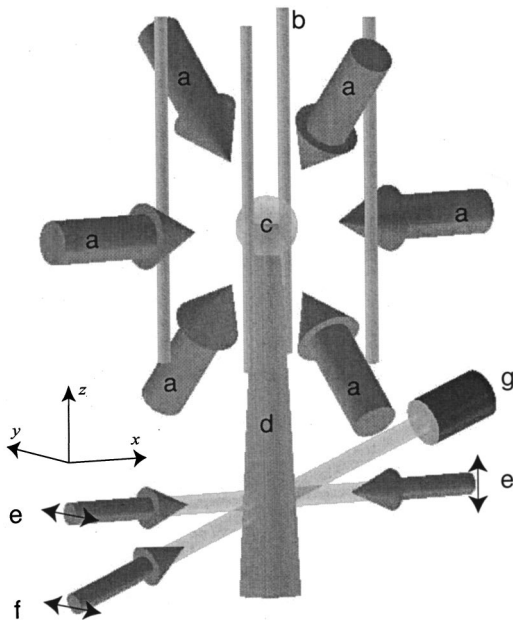


FIG. 2. Experimental setup. (a) Cooling beams of frequencies  $\omega_x = \omega_{45} - 2.5\Gamma$ ,  $\omega_{\text{up}} = \omega_x - \Delta$ , and  $\omega_{\text{down}} = \omega_x + \Delta$ . (b) 2D magnetic gradient wires. (c) Cold atomic source. (d) Continuous beam of cold atoms. (e) Pump beams of frequency  $\omega = \omega_{45} - 2.5\Gamma$ . (f) Probe beam of frequency  $\omega_p = \omega + \delta\omega$  where  $\delta\omega$  is swept in the range  $\pm 200$  kHz. (g) Photodetector. The pump and probe beams have linear polarizations. The angle between them has been exaggerated for the sake of clarity. In practice it is between  $1^\circ$  and  $2^\circ$ .

In the case of a beam, the dispersion curve is shifted by  $k\theta\bar{v}_z$ . Its center is a measure of the  $z$  component of the average velocity and its width is a measure of the longitudinal temperature. It can therefore be used as a beam velocimetry technique. To our knowledge this shifted RIR has never been observed before.

## II. EXPERIMENTAL SETUP

The experimental setup is represented on the diagram of Fig. 2. The upper part constitutes the source of the continuous beam. It has been described in detail in [10]. It consists of a 2D magneto-optical trap which confines the atoms in the  $Oxy$  plane but not in the vertical direction. The atoms are extracted from the trap by the moving molasses technique. The down-going (respectively, up-going) laser beams are frequency shifted by an amount  $+\Delta$  ( $-\Delta$ ) with respect to the frequency of the  $Ox$  beams. The theoretical launching velocity<sup>1</sup> is given by  $v_l = (\lambda/\cos\alpha)\Delta/2\pi$  where  $\lambda = 852.1$  nm and  $\alpha = \pi/4$ , therefore  $v_l = 1.205$  m s<sup>-1</sup> MHz<sup>-1</sup>. In this way we obtain a cesium beam with a flux of approximately  $10^8$  atoms per second, a temperature

<sup>1</sup>The actual launching velocity is slightly different because of the residual magnetic field and beam geometry imperfections. Moreover, the atomic beam local velocity differs from the launching velocity because of gravitation and radiation pressure.

between 50 and 300  $\mu\text{K}$ , and a velocity tunable from 1 to 12 m/s [10].

The laser beams used for the velocity distribution measurement are shown in the lower part of Fig. 2. The pump beam is retroreflected to avoid pushing atoms in the  $x$  direction. It is linearly polarized and, with the retroreflected beam, it forms a linearly cross-polarized (lin $\perp$ lin) molasses which cools the atoms in the  $x$  direction while heating them in the transverse directions. Its effect on the temperature measurement will be discussed further. The probe beam crosses the pump beam at a small angle  $\theta$  (between  $1^\circ$  and  $2^\circ$ ). Its polarization is linear and parallel with that of the copropagating pump beam. The two beams are derived from the same extended-cavity diode laser which is frequency stabilized a few linewidths below the  $F=4 \rightarrow F'=5$  hyperfine transition of the cesium  $D_2$  line. The pump intensity is between 5 and 30 mW/cm<sup>2</sup> and its frequency is  $\omega = \omega_{45} - 2.5\Gamma$  where  $\omega_{45}$  is the atomic transition frequency and  $\Gamma$  its natural width. The probe intensity is 0.1 mW/cm<sup>2</sup> and its frequency is  $\omega_p = \omega + \delta\omega$  where  $\delta\omega$  is in the range  $\pm 200$  kHz. To observe the RIR we sweep the probe beam frequency using an acousto-optic modulator and we record the transmitted intensity. The spectral resolution  $\delta\omega_{\text{res}}$  is limited by the sweep rate according to  $\delta\omega_{\text{res}}^2 \geq d(\delta\omega)/dt$  and by the transit time according to  $\delta\omega_{\text{res}} \geq 2\pi \times 0.62 v/d$ , where  $d$  is the Gaussian laser beam diameter. With the highest velocity of 4 m/s the transit time resolution is  $\delta\omega_{\text{res}} \approx 2\pi \times 1$  kHz. We have chosen the sweep rate  $d(\delta\omega)/dt < 2\pi \times 6$  kHz/ms so as not to weaken this resolution.

## III. EXPERIMENTAL RESULTS

Figure 3 displays the probe transmission spectrum for different probe polarizations for an atomic beam launched with a moving molasses of 1.205 m/s (1 MHz detuning). The spectra are the same as those observed by Verkerk *et al.* [5] in a 1D transient molasses but shifted to the left due to the overall beam velocity. They display amplification and absorption sideband resonances associated with stimulated Raman transitions between adjacent vibration levels along with a central resonant structure whose shape depends on probe polarization. When probe polarization is perpendicular to that of the copropagating pump beam [Fig. 3(a)] the cliff-shaped central structure is a Rayleigh resonance and when probe polarization is parallel to that of the copropagating pump beam [Fig. 3(b)] the dispersionlike central structure is a recoil induced resonance<sup>2</sup> [11,12]. Note that its amplitude is typically 0.3% of the transmitted intensity.

Figure 4 is an expanded view of Fig. 3(b); it displays the recoil-induced resonance observed on the probe transmission spectrum for the same atomic beam (1.205 m/s, 1 MHz de-

<sup>2</sup>In principle the recoil induced resonance is superimposed with a Rayleigh resonance. However, Guo has shown that in the parallel case the Rayleigh resonance is much weaker than the recoil induced resonance [11].

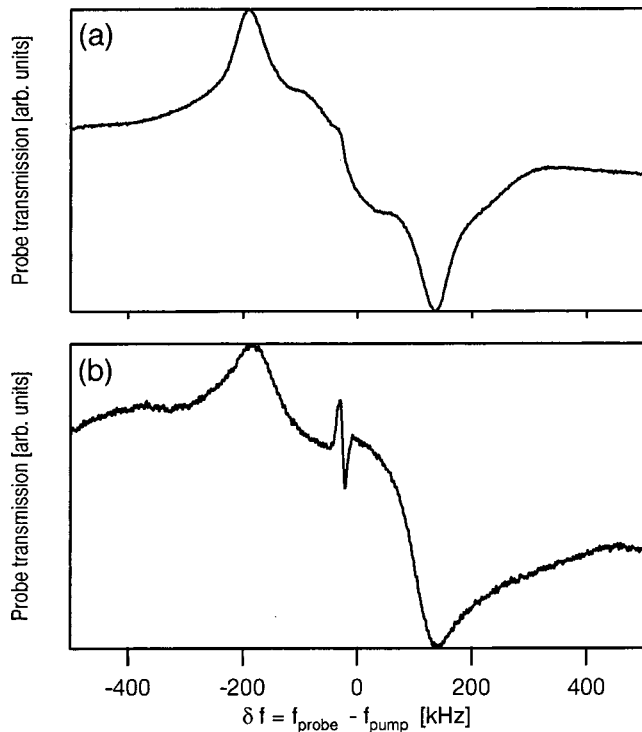


FIG. 3. Probe transmission spectrum in an atomic beam launched at 1.205 m/s (1 MHz detuning) for different probe polarizations. (a) Probe polarization perpendicular to that of the copropagating pump beam. (b) Probe polarization parallel to that of the copropagating pump beam.

tuning). As expected, it is a dispersionlike curve that represents the derivative of the atomic momentum distribution along the  $z$  direction. Its center is given by  $f_0 = k\theta\bar{v}_z/2\pi$  and the peaks are separated by  $\Delta f = 2k\theta\sqrt{k_B T/M}/2\pi$ . We have changed the angle  $\theta$  and the resonance width and center were observed to vary in accordance with the above formula. We can use  $f_0$  and  $\Delta f$  to get a measure of the mean velocity and

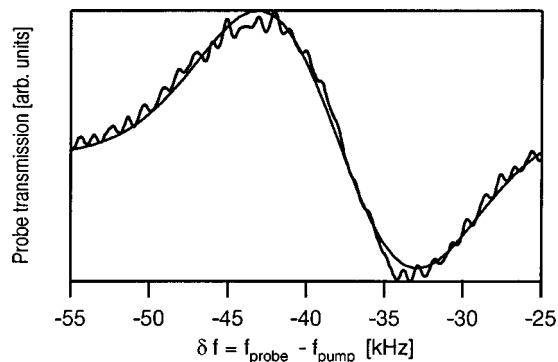


FIG. 4. Probe transmission spectrum in an atomic beam launched at 1.205 m/s (1 MHz detuning). We observe a recoil-induced resonance centered at  $-38$  kHz whose distance between peaks is approximately 10 kHz. The smooth line is a Gaussian derivative fit corresponding to a velocity  $\bar{v}_z = 1.3$  m/s and longitudinal temperature  $T = 510$   $\mu\text{K}$ .

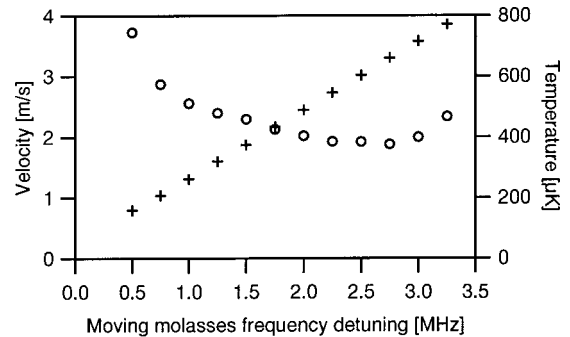


FIG. 5. Mean velocity  $\bar{v}_z$  (+) and longitudinal temperature  $T$  (O) of the atomic beam as a function of moving molasses detuning  $\Delta/2\pi$ . These values of  $\bar{v}_z$  and  $T$  have been computed from the center and distance between peaks of the RIR. They exhibit the same dependence on moving molasses detuning as the values obtained by TOF.

longitudinal temperature of the atomic beam. We obtain  $\bar{v}_z = 1.3$  m/s and  $T = 510$   $\mu\text{K}$ . The velocity thus obtained is slightly larger than the launching velocity, due to gravitation and fluorescence of the source which accelerate the atoms downwards. But the original beam temperature, approximately 70  $\mu\text{K}$  measured by TOF, is considerably increased by the transverse heating of the pump. We have observed that a slight misalignment of the cooling beams also affect  $\bar{v}_z$  and  $T$ .

We have measured the recoil-induced resonance for moving molasses detunings between 0.5 and 3.25 MHz (i.e., launching velocities between 0.6 and 3.9 m/s). Then we have computed  $\bar{v}_z$  and  $T$  using the above formula and the results are presented in Fig. 5. As expected these  $\bar{v}_z$  and  $T$  values have the same dependence on moving molasses detuning as those measured by TOF [10]. Note that we have repeated the same experiment for pump detunings between  $2\Gamma$  and  $10\Gamma$  and we have observed the same features.

#### IV. DISCUSSION

The mean velocity and longitudinal temperature of the atomic beam have also been measured by time of flight (TOF) [10]. When one takes account of the gravitation and the fluorescence of the source, the velocities measured by RIR are in agreement with those measured by TOF (relative error lower than 3%). Regarding the temperatures, those measured by RIR are higher because of the transverse heating caused by the pump. To evaluate this heating we have measured the temperature for various pump intensities. The results are presented in the graph of Fig. 6 for an atomic beam launched with a moving molasses of 1.205 m/s (1 MHz detuning). As expected the temperature increases with the pump intensity like the scattering rate of pump photons (the change in slope is due to saturation). This is in good agreement with a simple transverse heating model. To obtain the true atomic beam temperature (i.e., without heating) we

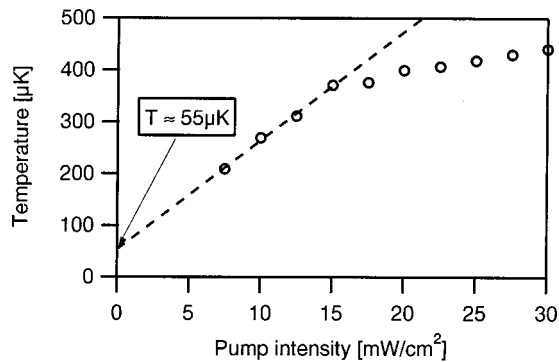


FIG. 6. Longitudinal temperature of the atomic beam as a function of pump intensity for an atomic beam launched with a moving molasses of 1.205 m/s (1 MHz detuning). As expected the temperature increases with pump intensity due to transverse heating. Extrapolation towards zero gives  $T \approx 55 \mu\text{K}$ , which is compatible with TOF results.

would have to gradually decrease the pump intensity down to zero. However, this is impossible because the RIR disappears when the pump intensity is too low. Nevertheless we can obtain an approximate value of the true temperature by extrapolating the curve towards  $I_{\text{pump}}=0$ . We thus obtain  $T \approx 55 \mu\text{K}$ , which is compatible with the value measured by TOF [10].

In principle, the observation of a RIR requires a free atomic motion in the transverse direction, which precludes velocity measurement in a 3D molasses. However, preliminary theoretical considerations suggest that the RIR should still be visible in the presence of a transverse friction force provided that  $k\theta\Delta v \gg \alpha/M$  where  $\alpha$  is the friction force coefficient and  $\Delta v$  is the velocity spread [13]. Therefore this method may be extended to measure atomic velocities in the center of the source of the continuous beam. In this case one uses one of the cooling beams (for example, the  $Ox$  beam) as a pump beam. Thus it is sufficient to add a probe beam and to record its transmission spectrum. The spectrum obtained is displayed in Fig. 7. It is more complicated because of the 3D

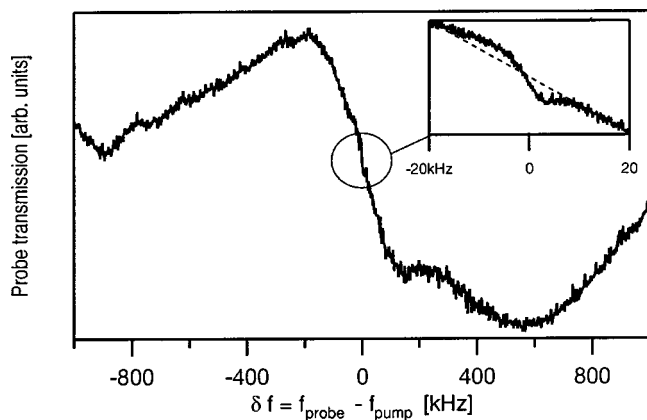


FIG. 7. Probe transmission spectrum in the 2D MOT source for zero-moving molasses frequency detuning. It is still possible to distinguish a small recoil-induced resonance in the spectrum center as shown in the inset.

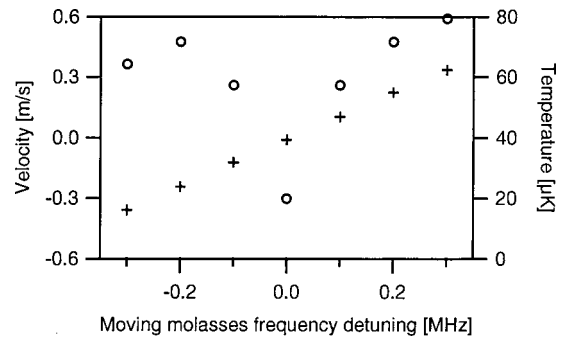


FIG. 8. Mean velocity  $\bar{v}_z$  (+) and longitudinal temperature  $T$  (O) in the cold atom source as a function of moving molasses detuning  $\Delta/2\pi$ . These values of  $\bar{v}_z$  and  $T$  have been computed from the center and distance between peaks of the RIR.

geometry of the cooling beams. Moreover,  $\sigma^+ - \sigma^-$  polarization gives place to wider Raman resonances. However, it is still possible to distinguish a small recoil-induced resonance in the spectrum center as shown in the inset. A displacement of this resonance is observed when one operates the source as a moving molasses. We have used the RIR center and width to evaluate the mean velocity and longitudinal temperature of the atoms in the source. The results are displayed in Fig. 8. They cannot be compared with TOF results because the domains of validity of the two techniques do not overlap. Indeed, for such small moving molasses frequency detunings ( $<0.5$  MHz) the TOF technique is not operational anymore and for bigger detunings ( $>0.5$  MHz) the RIR disappears, embedded by other resonances (Raman and Rayleigh). Nevertheless, we can compare the measured velocity with the theoretical launching velocity and we observe that they are in agreement (5% error). The measured temperature is lower in the source (Fig. 8) than in the atomic beam (Fig. 5) because the  $Ox$  cooling beam acts as the pump and consequently there is no more transverse heating. Therefore the RIR measurement gives directly the true longitudinal temperature of the atoms in the source. The graph of Fig. 8 shows that the temperature reaches a minimum for zero moving molasses frequency detuning. This result is new evidence of the already observed heating caused by the moving molasses.

## V. CONCLUSION

We have observed Raman, Rayleigh, and recoil-induced resonances in a continuous beam of slow and cold cesium atoms. We have shown that one can use the recoil-induced resonance to measure the velocity distribution of the atomic beam. The center of the distribution gives a measure of the average velocity which is in agreement with the result obtained by TOF. The width of the distribution gives a measure of the longitudinal temperature which is higher than the temperature measured by TOF. The difference is explained by the transverse heating caused by the pump. We have measured this heating and when it is subtracted from the RIR temperature one finds the temperature measured by TOF.

Compared to TOF, this velocimetry technique has the ad-

vantage of being local, more sensitive in the low-velocity regime ( $v < 1$  m/s) and it gives access to transverse velocities and temperatures. In addition it may be extended to measure atomic velocities in the center of the source. Therefore it could be used to get a detailed map of velocities and temperatures of the atomic beam along with its source.

## ACKNOWLEDGMENTS

We would like to thank Y. Castin for helpful discussions and C. Salomon for suggesting us to use this velocimetry technique. This work was supported by the Swiss National Science Foundation.

- [1] J. Tabosa *et al.*, Phys. Rev. Lett. **66**, 3245 (1991).
- [2] D. Grison *et al.*, Europhys. Lett. **15**, 149 (1991).
- [3] J.-Y. Courtois and G. Grynberg, Phys. Rev. A **46**, 7060 (1992).
- [4] J.-Y. Courtois and G. Grynberg, Phys. Rev. A **48**, 1378 (1993).
- [5] P. Verkerk *et al.*, Phys. Rev. Lett. **68**, 3861 (1992).
- [6] B. Lounis *et al.*, Phys. Rev. Lett. **69**, 3029 (1992).
- [7] J. Guo, P.R. Berman, and B. Dubetsky, Phys. Rev. A **46**, 1426 (1992).
- [8] D.R. Meacher *et al.*, Phys. Rev. A **50**, R1992 (1994).
- [9] J.-Y. Courtois, G. Grynberg, B. Lounis, and P. Verkerk, Phys. Rev. Lett. **72**, 3017 (1994).
- [10] P. Berthoud, E. Fretel, and P. Thomann, Phys. Rev. A **60**, R4241 (1999).
- [11] J. Guo, Phys. Rev. A **49**, 3934 (1994).
- [12] J.-Y. Courtois and G. Grynberg, Adv. At., Mol., Opt. Phys. **36**, 87 (1996).
- [13] Y. Castin (private communication).